SIAM J. APPL. MATH.
Vol. 72, No. 2, pp. 577–593

EXTRACTING SOLITONS FROM NOISY PULSES*

JINGLAI LI† AND WILLIAM L. KATH‡

Abstract. We describe an iterative method that extracts the underlying soliton from a noisy pulse. The method is formulated as a functional iteration: at each step, the soliton component of the difference between the noisy pulse and the current underlying soliton is determined via soliton perturbation theory; this is then added to the soliton, and the process is repeated. We show that this iteration converges if the perturbation is not too large, and we give the specific types of deviations which most easily cause the iteration to fail to converge. As an example of the method's use, we apply it to obtain improved statistics of the amplitude, phase, frequency, and position of a soliton propagating in an optical fiber in the presence of amplifier noise.

Key words. soliton, perturbation theory, nonlinear Schrödinger equation, optical fiber communication system, functional iteration, amplifier noise

AMS subject classifications. 35C08, 35Q55, 35R60, 65H10

DOI. 10.1137/110828289

1. Introduction.

A fundamental characteristic of a soliton is its ability to maintain its identity when perturbed. For example, solitons collide and pass through one another without permanent change of shape [46] and resist effects due to noise [15]. The robustness of solitons to perturbations, which is known to arise from the integrability of the nonlinear partial differential equations (PDEs) possessing soliton solutions [3, 47], is a main motivation of interest in such pulses. Because of these properties, solitons are often used as a prototypical model for pulses in optical fibers or mode-locked lasers; see, for example, [1, 2, 4, 13, 17, 27].

At the same time, of course, solitons are not completely immune to all perturbations. The nonlinear PDEs governing soliton propagation typically possess several invariances (such as with respect to changes in position or time), and by Noether's theorem each invariance is associated with a conserved quantity [10, 45]. Each of these quantities, of course, must also be constant for a soliton solution, and thus that solution possesses an independent set of parameters directly related to them. These soliton parameters are determined solely by the initial conditions, and so any perturbation that changes them produces an equally valid solution. As a result, for soliton solutions there is no resistance to perturbations in functional directions associated with the invariances, and such perturbations can accumulate during propagation [6, 20, 29].

Perturbation theory for nonlinear evolution equations possessing soliton solutions [3, 19, 23, 26] is thus often separated into two main components—perturbations to the soliton via changes in its parameters, and perturbations in the nonsoliton part of the solution (also known as dispersive radiation). The soliton part of the perturbation theory can be performed in a number of ways. For example, one can linearize around a

*Received by the editors March 22, 2011; accepted for publication (in revised form) January 17, 2012; published electronically April 12, 2012. The work was supported by National Science Foundation grant DMS-0709070.
http://www.siam.org/journals/siap/72-2/82828.html
†Department of Aeronautics and Astronautics, Massachusetts Institute of Technology, Cambridge, MA 02139 (jinglai@mit.edu).
‡Department of Engineering Sciences and Applied Mathematics, Northwestern University, Evanston, IL 60208 (kath@northwestern.edu).

soliton and project with the eigenfunctions of the linearized equation [6, 12, 21, 25, 29] to obtain the perturbation equations; since one typically knows how the solitons depend upon the parameters, the corresponding solutions of the linearized equation are known immediately. Alternatively, one can use inverse scattering [3, 19, 23, 24] to derive the effect of perturbations upon the soliton part of the solution. Changes to the soliton parameters can also be obtained by constructing the averaged Lagrangian associated with the nonlinear evolution equation [25, 30, 45], or by employing the conservation laws associated with the equation [20, 23]. The perturbation equations for the continuum (i.e., the dispersive radiation) can similarly be obtained from the linearized equation [11, 16, 21, 22] or from inverse scattering [19, 23]. Of course, because of the rich mathematical structure associated with such equations, there are many connections between these different methods.

The separation of the effects of perturbations into those on solitons and effects on dispersive radiation can also be done numerically. In this context, the main method is a numerical implementation of the Zakharov–Shabat (ZS) spectral problem [7, 44], since the eigenvalues of the direct spectral problem correspond directly with the solitons [9, 47]. As is the case with analytic perturbation theory, significant information about the dynamics of solutions can be obtained by following the solitons and dispersive radiation numerically [37].

We consider here the case where solitons are perturbed by additive noise. Such perturbations are common in a number of contexts, such as the propagation of solitons in nonlinear optical fibers. In one case, gain is used to compensate loss in the fiber, and noise is added by the amplifiers [5, 13, 17]. This additive noise can be broad in both the spectral and temporal domains, leading to difficulties when one wishes to compare analytical and numerical solutions of such randomly perturbed solitons.

The main difficulty arises when performing such comparisons because one must separate the soliton from the noise. This happens automatically for the analytical solutions, because the methods focus on the perturbed soliton, but for direct comparison this should also be done in the numerical solution. Solving the ZS spectral problem separates the soliton from the noise, but this is computationally expensive. The efficiency of the numerical method is particularly important: when one models the effects of noise one is likely to be interested in determining statistics, and thus Monte Carlo (MC) simulations are typically performed. In such cases, many statistical samples are usually needed in order for means, variances, and other appropriate measures to be computed to sufficient accuracy, and the relative speed of the numerical method is then multiplied by a large factor. This motivates the main result of this paper, which is an iterative method that can *efficiently* and *accurately* recover the soliton part of a noisy pulse. This method is almost as accurate as solving the ZS eigenvalue problem but is considerably faster.

The outline of the paper is as follows. Section 2 discusses, in the context of optical solitons, some of the issues that arise when one considers additive noise. Section 3 then describes the iterative soliton extraction method in detail and discusses the issue of convergence. Section 4 explains how to determine the "worst" perturbation directions associated with the iterative method, i.e., the types of perturbations which most easily cause convergence to fail. Finally, section 5 provides an example application of the method, and section 6 offers some final discussion.

2. Optical solitons in the presence of noise. The basic equation governing pulse dynamics in an optical fiber is the cubic nonlinear Schrödinger equation (NLSE)

[4, 5, 13, 14]

$$i\frac{\partial u}{\partial t} + \frac{1}{2}\frac{\partial^2 u}{\partial x^2} + |u|^2 u = 0. \tag{2.1}$$

In (2.1), u is the envelope of the optical field, t represents propagation distance, and x represents retarded time[1] [4, 5, 13, 14]. In this model, solitons are hyperbolic-secant pulses that perfectly preserve their shape during propagation, i.e., $u_s(x,t) = u_0(x,t)\, e^{i\Theta}$ with

$$u_0(x,t) = A\,\mathrm{sech}(A(x - X(t)))\,, \qquad \Theta = \Omega(x - X(t)) + \Phi(t)\,. \tag{2.2}$$

Here A and Ω are the soliton amplitude and frequency, while $X(t)$ and $\Phi(t)$ are the position and phase at the center of the soliton. A and Ω are constant, while $dX/dt = \Omega$ and $d\Phi/dt = (A^2 + \Omega^2)/2$.

Because it neglects various higher-order physical effects such as third-order dispersion, Raman scattering, and polarization-mode dispersion (PMD) [4, 5], the cubic NLSE provides only an approximate description of the actual propagation of optical pulses in a fiber. In addition, it neglects the amplified spontaneous emission (ASE) noise added by in-line optical amplifiers [5, 13, 17]. In real-world systems, therefore, solitons can be perturbed in a number of different ways. In addition, several perturbations are random.

ASE noise is different from many of the other perturbations because it is additive; i.e., noise accumulates even in the absence of a pulse. ASE noise is often modeled by assuming that a random term is added at each amplifier [17], i.e.,

$$\frac{\partial u}{\partial t} = \frac{i}{2}\frac{\partial^2 u}{\partial x^2} + i|u|^2 u + \sum_{n=1}^{N_a} s_n(x)\,\delta(t - t_n)\,. \tag{2.3}$$

Here N_a is the number of amplifiers, t_n are the locations of amplifiers, and $\delta(t)$ is the Dirac delta distribution. The added terms $s_n(x)$ are taken to represent independent and identically distributed (i.i.d.) white Gaussian noise satisfying

$$\mathbb{E}[s_n(x)] = 0\,, \qquad \mathbb{E}[s_n(x) s_{n'}^{\dagger}(x')] = \sigma^2 \delta(x - x')\,\delta_{nn'}, \tag{2.4}$$

where $\mathbb{E}[\,\cdot\,]$ denotes ensemble average, $\delta(x - x')$ is a Dirac delta in the same coordinate as the pulse profile, $\delta_{nn'}$ is the Kronecker delta, and σ^2 is a combination of physical constants and system parameters that determines the noise power [17]. Technically speaking, (2.4) is not correct as written, since it implies an infinite noise bandwidth and thus produces an infinite noise power; any physical system (or any numerical computation) necessarily has a finite noise bandwidth [31]. When calculating amplitude, frequency, and timing fluctuations, however, the specific value of the noise bandwidth is unimportant as long as it is larger than the soliton bandwidth (which is the case in practice), because only those components of the noise within the same spectral range as the pulse affect these soliton parameters. The noise bandwidth *does* directly affect the phase fluctuations, however, and thus when simulations dealing with phase are performed the numerical bandwidth (i.e., the number of Fourier modes used for the additive noise) should also be reported [8].

[1] In the above and in what follows, we will use the mathematically more familiar context of t as an evolution variable and x as a variable associated with the pulse profile, even though in the context of optical fibers evolution is with respect to distance and the pulse profile is with respect to time.

To better understand the difficulties that arise when comparing numerical simulations and analytical results from perturbation theory, consider the example of determining the amplitude of a propagating soliton that is perturbed by noise. At the nth amplifier, the first-order change in the soliton amplitude induced by the random perturbation $s_n(x)$ is determined by projecting this perturbation onto the adjoint mode of the NLSE linearized around the soliton [17, 32, 33].

$$\Delta A_n = \mathrm{Re} \int_{-\infty}^{\infty} u_0(x, t_n)\, e^{-i\Theta} s_n(x)\, dx. \tag{2.5}$$

The perturbation to the amplitude ΔA_n is a linear combination of Gaussian random variables and so is Gaussian itself. And because the noise and the solution to which it is being added are independent, from (2.4) we have [17, 32, 33]

$$\langle \Delta A_n \rangle = 0 \quad \text{and} \quad \langle (\Delta A_n)^2 \rangle = \frac{\sigma^2}{2} \int_{-\infty}^{\infty} |u_0|^2\, dx = \sigma^2 A_n, \tag{2.6}$$

where A_n is the amplitude of the soliton just before the amplifier. Thus, within the approximation of soliton perturbation theory (SPT) (i.e., if the change at each amplifier is small) the amplitude obeys the difference equation [33]

$$A_{n+1} = A_n + \sigma \sqrt{A_n}\, z_n, \tag{2.7}$$

where the z_n are i.i.d. standard Gaussian random variables. From this one finds

$$\langle A_{n+1} \rangle = \langle A_n \rangle \quad \Rightarrow \quad \langle A_n \rangle = A_0 \tag{2.8}$$

and

$$\langle A_{n+1}^2 \rangle = \langle A_n^2 \rangle + \sigma^2 \langle A_n \rangle \quad \Rightarrow \quad \langle A_n^2 \rangle = A_0^2 + n\sigma^2 A_0. \tag{2.9}$$

Thus, the prediction is that the variance of A_n should grow linearly with distance (i.e., n).

Since the above analysis is the result of first-order perturbation theory and is only approximate for small amounts of noise, it is natural to verify its accuracy via numerical solutions. To the same first-order accuracy as SPT, a conservation law can be used to compute the soliton amplitude approximately [20, 23]:

$$A_n = \frac{1}{2} \int_{-\infty}^{\infty} |u(x, t_n)|^2\, dx. \tag{2.10}$$

This equation is exact when there is no perturbation and u is a soliton, of course. Unfortunately, when (2.10) is used in an actual numerical simulation, the results are not as expected, as shown in Figure 2.1. One obvious problem is that instead of the mean amplitude being approximately constant, it grows strongly with distance.

The explanation of this discrepancy is seen immediately if one plots the pulse profile at a fixed t, as shown in Figure 2.2. In particular, not only is the soliton significantly perturbed, but in addition a considerable amount of noise has been added to the regions in which the solution intensity was originally negligible. Thus, although the perturbation is small pointwise (one can see from (2.10) that it is of second order), including its contribution over a large computational window can lead to a significant discrepancy between theory and computations. This is also apparent in previous

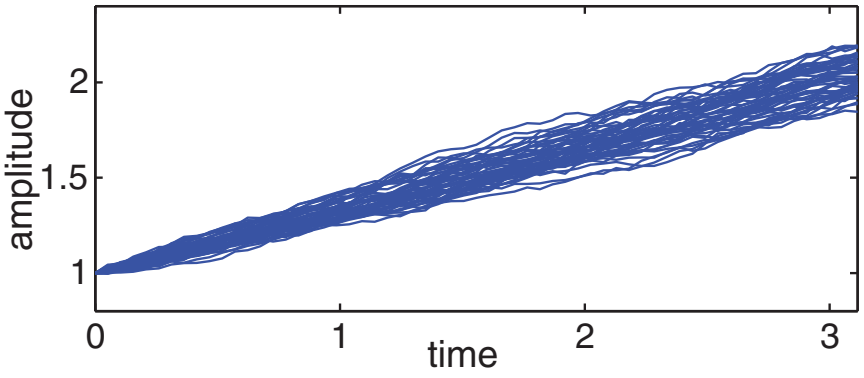

FIG. 2.1. *Soliton amplitude determined using* (2.10)*, displayed as it evolves. For this simulation, independent Gaussian noise with* $\sigma^2 = 7 \times 10^{-4}$ *is added to the pulse every* 0.052 *units during propagation. The computational window is* 23.4 *units wide and fifty random trials are shown.*

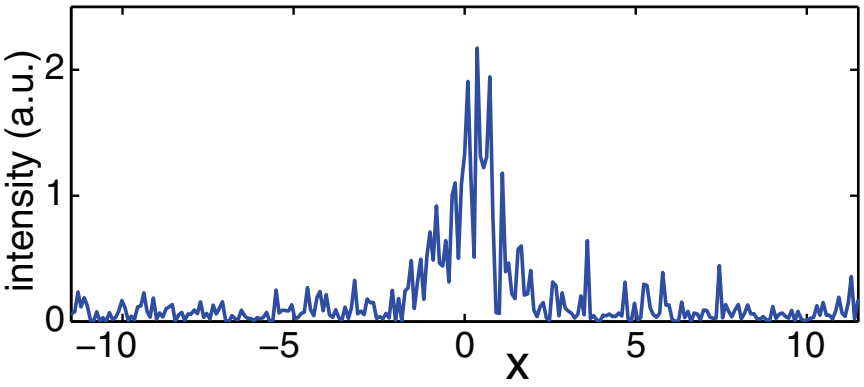

FIG. 2.2. *Pulse intensity profile at* $t = 3.12$ *for one trial of the simulations shown in Figure* 2.1.

results; for example, if one compares the result of perturbation theory for the soliton amplitude in the presence of noise [13, 17] with the result of perturbation theory for the total energy in a finite-time window [31], the answers differ by a term proportional to both the width of the time window and the noise variance, i.e., by the additional energy that is being contributed from the background noise over the entire interval.

The above problems persist when one attempts to compute the other soliton parameters from numerical solutions via conservation laws or their moments:

$$\Omega_n = \frac{i}{2A_n} \int (u u_x^* - u^* u_x)\, dx, \tag{2.11a}$$

$$X_n = \frac{1}{A_n} \int x|u|^2\, dx, \tag{2.11b}$$

$$\Phi_n = \frac{1}{A_n} \int \arctan(\operatorname{Im} u / \operatorname{Re} u)|u|^2\, dx. \tag{2.11c}$$

(Above and in what follows, all integrals are assumed to be complete unless stated otherwise.) Various formulas can be used to determine the soliton phase; (2.11c) is one natural choice. The phase obtained depends, to a certain extent, upon the formula employed, however [39]. In addition, a variant of the above is to first apply a band-

pass filter to u and then to substitute the filtered pulse instead of the original one into (2.10) and (2.11) to calculate the parameters [33]. The filter, of course, reduces the effect of the added noise upon the final parameters. This modified moment method is efficient, but it is not always as accurate as desired, as sometimes its results deviate significantly from the true soliton parameters, especially when the noise component is not very small compared to the soliton. In addition, several parameters must be tuned in this method, such as the width of the filter and the width of the window around the pulse that is used to compute the moments, and the results depend strongly on their values. For example, if the filter used is too strong, some of the soliton will be thrown away along with the noise.

A more accurate method of extracting the underlying soliton is to solve the ZS eigenvalue problem [7, 33, 44]. The ZS problem has the form

$$v'(x) + i\zeta v(x) = u(x,t_n)w(x), \qquad w'(x) - i\zeta w(x) = -u^*(x,t_n)v(x), \tag{2.12}$$

where $v(x)$ and $w(x)$ are known as Jost functions. Using the noisy pulse as the potential $u(x,t_n)$ in (2.12), one solves this eigenvalue problem numerically and reconstructs a "clean" underlying soliton from the Jost functions [33]. This method is accurate but computationally expensive because it is equivalent to determining selected eigenvalues and eigenfunctions of a large matrix. In applications which require a large number of such simulations, such as when performing MC simulations to study the statistics of transmission errors [33, 34, 40, 41], the computational cost of this method can become prohibitive.

3. Soliton extraction via perturbation theory and functional iteration. The method described here for extracting a soliton from a noisy signal is based on SPT. Suppose that $u_s(x,t)$ as given in (2.2) is the approximate soliton part of the noisy pulse $u(x,t)$. The idea is to consider $\Delta u(x,t) = u(x,t) - u_s(x,t)$ as a perturbation of $u_s(x,t)$ and to determine the correction to the soliton parameters from it. In what follows we will omit the arguments x and t and the subscript n if this does not cause ambiguity. According to SPT, the perturbation Δu causes changes in the soliton parameters which can be determined by projecting it onto the adjoint modes of the linearized NLSE [13, 17, 20, 21, 33], i.e.,

$$\Delta A = \mathrm{Re}\int e^{-i\Theta}\,\underline{v}_A^\dagger\,\Delta u\,dx, \tag{3.1a}$$

$$\Delta \Omega = \mathrm{Re}\int e^{-i\Theta}\,\underline{v}_\Omega^\dagger\,\Delta u\,dx, \tag{3.1b}$$

$$\Delta X = \mathrm{Re}\int e^{-i\Theta}\,\underline{v}_X^\dagger\,\Delta u\,dx, \tag{3.1c}$$

$$\Delta \Phi = \mathrm{Re}\int e^{-i\Theta}\,(\underline{v}_\Phi^\dagger - X\,\underline{v}_\Omega^\dagger)\,\Delta u\,dx, \tag{3.1d}$$

where † stands for the complex conjugate and where

$$\underline{v}_A = u_0, \qquad \underline{v}_\Omega = -\frac{1}{A} i \frac{\partial u_0}{\partial x},$$

$$\underline{v}_X = -\frac{1}{A}(x-X)\,u_0, \qquad \underline{v}_\Phi = \frac{1}{A} i \frac{\partial}{\partial x}[(x-X)\,u_0]$$

are the adjoint modes of the NLSE linearized around a soliton.

To simplify the notation, we introduce the vector $\vec{P} = (A, \Omega, X, \Phi)^T$ where the superscript means transpose; then (3.1) becomes $\Delta\vec{P} = \vec{F}(\vec{P})$. By definition,

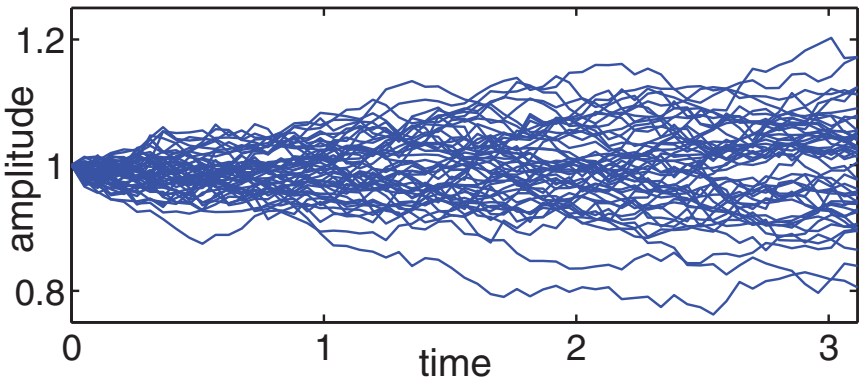

FIG. 3.1. *Soliton amplitude determined using the function iteration, displayed as a function of time. The simulation parameters for these* 50 *trials are the same as in Figure* 2.1.

this equation determines the change in the soliton parameters associated with the perturbation Δu; since we are starting with a set of parameters, the right-hand side depends upon these values. If the underlying soliton has been chosen correctly, though, then the changes to the parameters are zero and one has $\vec{F}(\vec{P}) = 0$.

If the soliton parameters have not been accurately determined, however, we can interpret the perturbation equations $\Delta\vec{P} = \vec{F}(\vec{P})$ as the functional iteration [18, 42] $\vec{P}_{n+1} - \vec{P}_n = \vec{F}(\vec{P}_n)$ and apply it repeatedly until a desired level of accuracy is obtained. Thus, we have the following algorithm to determine the soliton parameters:

1. Let $n = 0$; choose an error tolerance τ; find an initial point $\vec{P}_0$.
2. Compute $\vec{P}_{n+1} = \vec{P}_n + \Delta\vec{P}_n$, where $\Delta\vec{P}_n = \vec{F}(\vec{P}_n)$.
3. Stop if $\|\Delta\vec{P}_n\|_2 < \tau$; otherwise, let $n = n + 1$ and go to step 2.

One expects, of course, that the iteration will only converge to the correct solution if the initial guess $\vec{P}_0$ is sufficiently close to a root. Therefore, an important issue associated with implementing the functional iteration is to find a good initial estimate of the soliton parameters. The filtered moment method given by (2.10) and (2.11) provides reasonable estimates for A, Ω, and X, but unfortunately the pulse phase estimated by the moment method can be fairly poor. Because of this, we first obtain A_0, Ω_0, and X_0 as initial estimates of A, Ω, and X using (2.10) and (2.11), and we then seek the Φ_0 that minimizes $\|\Delta u\|_2 = \int |u - u_s(A_0, \Omega_0, X_0, \Phi_0)|^2 dx$. Fortunately, this problem has a simple explicit solution, namely,

$$\Phi_0 = \arg \int u \operatorname{sech}(A_0(x - X_0)) e^{-i\Omega_0(x - X_0)}\, dx. \tag{3.2}$$

As a brief example of the utility of the method, in Figure 3.1 we show the same simulation as for Figure 2.1, but this time with the soliton amplitude determined via the functional iteration rather than the conservation law (2.10). It is now seen that the mean amplitude is approximately constant, as predicted by (2.8). In addition, the variance appears to grow with distance as predicted by (2.9). More detailed results for the growth of the variance are given in section 5.

4. Conditions for convergence. Suppose $\vec{P}^* = (A^*, \Omega^*, X^*, \Phi^*)$ is a root of $\vec{F}(\vec{P})$=0, the initial point $\vec{P}_0$ is in a neighborhood $N(\vec{P}^*)$ of $\vec{P}^*$, and $\epsilon_n = \|\vec{P}^* - \vec{P}_n\|_2$ is the distance between $\vec{P}_n$ and $\vec{P}^*$. Then the error $\vec{E}_n = \vec{P}_n - \vec{P}^* = \epsilon_n(e_A, e_\Omega, e_X, e_\Phi)$,

where $(e_A, e_\Omega, e_X, e_\Phi)$ is a unit vector. It follows that

$$\vec{E}_{n+1} = \vec{P}_{n+1} - \vec{P}^* = \vec{P}_n + \vec{F}(\vec{P}_n) - \vec{P}^* = \vec{E}_n + \vec{F}(\vec{P}_n) = \vec{E}_n + \vec{F}(\vec{P}^* + \vec{E}_n). \tag{4.1}$$

Expanding $\vec{F}(\vec{P}^* + \vec{E}_n)$ in powers of ϵ_n yields

$$\vec{F}(\vec{P}_n) = \vec{F}(\vec{P}^*) + \left.\frac{\partial \vec{F}(\vec{P})}{\partial \vec{P}}\right|_{\vec{P}=\vec{P}^*} \vec{E}_n + O(\epsilon_n^2)\,. \tag{4.2}$$

In addition, the elements of the Jacobian matrix in the second term on the right-hand side of (4.2) can be written as

$$\begin{aligned}\left.\frac{\partial F_j(\vec{P})}{\partial P_k}\right|_{\vec{P}=\vec{P}^*} = &-\operatorname{Re}\int e^{-i\Theta}(\underline{v}_j^\dagger - \delta_{j,\Phi} X\, \underline{v}_\Omega^\dagger)\left.\frac{\partial u_s}{\partial P_k}\right|_{\vec{P}=\vec{P}^*} dx \\ &+ \operatorname{Re}\int \frac{\partial}{\partial P_k}[e^{-i\Theta}(\underline{v}_j^\dagger - \delta_{j,\Phi} X\, \underline{v}_\Omega^\dagger)]\,\Delta u^*\, dx,\end{aligned} \tag{4.3}$$

where P_j and P_k are A, Ω, X, or Φ and $\delta_{j,k}$ is the Kronecker delta $\delta_{j,k}$=1 if j=k and $\delta_{j,k}$=0 if $j \neq k$. Also note that $\Delta u^* = u - u_s(\vec{P}^*)$ must be purely dispersive; i.e., since $\vec{P}^*$ determines the underlying soliton, the projections of the remaining perturbation along each of the directions given by the modes of the linearized NLSE must be zero.

Recall that the derivatives of u_s with respect to the soliton parameters are connected to the linear modes via

$$\frac{\partial u_s}{\partial A} = e^{i\Theta} v_A, \quad \frac{\partial u_s}{\partial \Omega} = e^{i\Theta}\,(v_\Omega + X v_\Phi), \quad \frac{\partial u_s}{\partial X} = e^{i\Theta} v_X, \quad \frac{\partial u_s}{\partial \Phi} = e^{i\Theta} v_\Phi. \tag{4.4}$$

Recall also that the linear modes are orthonormal: $\langle \underline{v}_j, v_k \rangle = \operatorname{Re}\int \underline{v}_j^\dagger\, v_k\, dx = 1$ if $j = k$ and is zero otherwise. These facts, along with (4.3) and (4.4), yield

$$\vec{F}(\vec{P}_n) = -\vec{E}_n + \mathsf{J}(\vec{P}^*)\vec{E}_n + O(\epsilon_n^2), \tag{4.5}$$

where $\mathsf{J} = \{a_{jk}\}$, and $a_{jk} = \operatorname{Re}\int(\partial[e^{-i\Theta}(\underline{v}_j^\dagger - \delta_{j\,\Phi} X\, \underline{v}_\Omega^\dagger)]/\partial P_k)\,\Delta u^*\, dx$. Substituting (4.5) into (4.1) and neglecting higher order terms, one obtains

$$\vec{E}_{n+1} = \mathsf{J}(\vec{P}^*)\vec{E}_n. \tag{4.6}$$

Standard results [38] then imply that the iterates converge to the root $\vec{P}^*$ if $\rho(\mathsf{J}(\vec{P}))$<1 for all $\vec{P} \in N(\vec{P}^*)$, where $\rho(\mathsf{J})$ is the spectral radius [28, 43] of J.

Note that J is a 4×4 matrix whose coefficients are determined by forming the inner products between the derivatives of the adjoint modes of the linearized NLSE with respect to the soliton parameters and the deviation between the initial pulse and the soliton at the fixed point (i.e., the residual perturbation). Because the magnitude of the coefficients scales with the size of Δu^*, a large enough perturbation will always make the convergence fail, as long as not all of the inner products are zero.

The method applies to an arbitrary fixed point soliton, of course. Because of the invariances of the NLSE, however, it is not necessary to examine how the algorithm's convergence depends upon all parameters. To show this, we define

$$\zeta = A^*(x - X^*) \tag{4.7a}$$

and

$$a_n = \frac{A_n}{A^*}, \quad \xi_n = A^*(X_n - X^*), \quad \omega_n = \frac{\Omega_n - \Omega^*}{A^*}, \quad \phi_n = \Phi_n - \Phi^*, \tag{4.7b}$$

where, as a reminder, A^*, Ω^*, X^*, and Φ^* are the values of the parameters at the fixed point. It follows that

$$\Theta = \Omega_n(x - X_n) + \Phi_n = \Theta^* + \theta_n, \tag{4.8}$$

where

$$\Theta^* = \omega^*\zeta + \Phi^*, \quad \omega^* = \Omega^*/A^*, \quad \theta_n = \omega_n(\zeta - \xi_n) - \omega^*\xi_n + \phi_n. \tag{4.9}$$

Substituting (4.7) and (4.8) into (3.1), after some manipulation one finds

$$\Delta a_n = \mathrm{Re} \int a_n \,\mathrm{sech}(a_n(\zeta - \xi_n)) \left[e^{-i\theta_n} u_*(\zeta) - a_n \,\mathrm{sech}(a_n(\zeta - \xi_n))\right] d\zeta, \tag{4.10a}$$

$$\Delta\omega_n = \mathrm{Re} \int -i\frac{\partial}{\partial\zeta} \,\mathrm{sech}(a_n(\zeta - \xi_n)) \left[e^{-i\theta_n} u_*(\zeta) - a_n \,\mathrm{sech}(a_n(\zeta - \xi_n))\right] d\zeta, \tag{4.10b}$$

$$\Delta\xi_n = \mathrm{Re} \int -(\zeta - \xi_n) \,\mathrm{sech}(a_n(\zeta - \xi_n)) \left[e^{-i\theta_n} u_*(\zeta) - a_n \,\mathrm{sech}(a_n(\zeta - \xi_n))\right] d\zeta, \tag{4.10c}$$

$$\Delta\phi_n = \mathrm{Re} \int i\frac{\partial}{\partial\zeta}[\zeta \,\mathrm{sech}(a_n(\zeta - \xi_n))] \left[e^{-i\theta_n} u_*(\zeta) - a_n \,\mathrm{sech}(a_n(\zeta - \xi_n))\right] d\zeta, \tag{4.10d}$$

where

$$u_*(\zeta) = e^{-i\Theta^*} \frac{1}{A^*} u\left(\frac{\zeta}{A^*} + X^*\right). \tag{4.11}$$

The fixed point of this rescaled iteration is, of course, $a = 1$, $\xi = 0$, $\omega = 0$, and $\phi = 0$. In addition, $u_*(\zeta)$ is just a rescaled version of the perturbed pulse; since this pulse is arbitrary, its dependence on the soliton parameters at the fixed point is spurious and can be ignored. The only remaining dependence upon the soliton parameters at the fixed point in the iteration given by (4.10) is upon $\omega^* = \Omega^*/A^*$ (through θ_n). Thus, the spectral radius (and whether or not the iteration converges) depends upon the soliton parameters only through ω^*.

As stated previously, when $\rho(\mathsf{J}(\vec{P}^*)) \geq 1$, the algorithm can be expected to diverge, no matter how good the initial guess is [36]. Because the coefficients of J depend upon inner products between the perturbation and the derivatives of the adjoint modes with respect to the soliton parameters, however, it is clear that certain perturbations will be better or worse than others. Thus, to assess the robustness of the method, it is useful to identify the *worst perturbation direction*, in the sense that it leads to the largest $\rho(\mathsf{J})$ for a given amount of noise energy. Alternatively, a perturbation in this direction will produce the minimal noise energy that leads to a failure of convergence (i.e., $\rho(\mathsf{J}) \geq 1$). Furthermore, if the noise energy is smaller than the minimal failure value determined by this worst perturbation direction, the algorithm will converge for *all* perturbations.

Identifying the worst perturbation direction can be formulated as a constrained optimization problem: we wish to maximize $\rho(\mathsf{J})$ with respect to Δu, subject to $\|\Delta u\|_2 = 1$. Recalling that $a_{jk} = \mathrm{Re} \int (\partial[e^{-i\Theta}(\underline{v}_j^\dagger - \delta_{j\,\Phi} X\, \underline{v}_\Omega^\dagger)]/\partial P_k)\, \Delta u^*\, dx$, the worst perturbation Δu must be a linear combination of these functions, namely,

$$\Delta u = \sum_j \sum_k b_{jk} \partial(e^{i\Theta} \underline{v}_j)/\partial P_k, \tag{4.12}$$

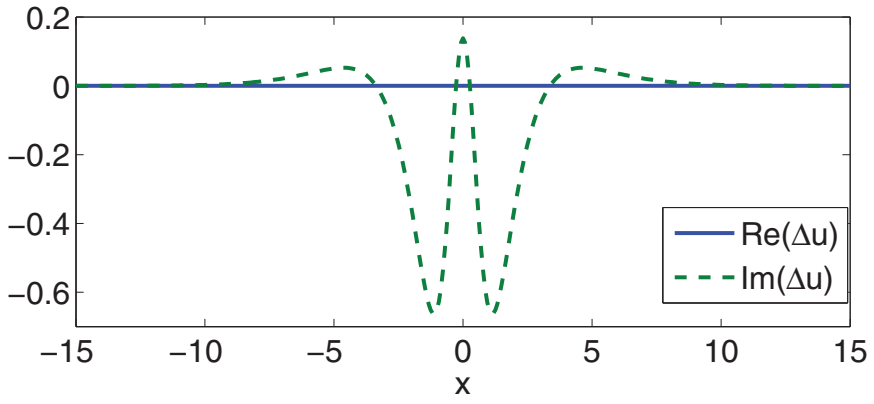

FIG. 4.1. *The worst perturbation direction for soliton* $u(x) = \mathrm{sech}(x)$*, obtained using the method described in the text.*

where b_{jk} are coefficients and P_j and P_k are A, Ω, X, or Φ. In addition, another constraint must be satisfied: the projection of Δu on the adjoint mode directions $\underline{v}_l$ must be zero, i.e.,

$$\mathrm{Re}\int \underline{v}_l \Delta u = 0, \tag{4.13}$$

since the perturbation cannot change the fixed point soliton parameters. Substituting (4.12) into (4.13) then yields

$$\sum_j \sum_k \left(\mathrm{Re}\int \underline{v}_l^\dagger \frac{\partial \underline{v}_j}{\partial P_k}\, dx \right) b_{jk} = 0. \tag{4.14}$$

Not all of the functions in (4.12) are linearly independent. In fact, as can be verified analytically, only twelve functions are linearly independent, and, in addition, all the adjoint modes v_j are contained in the space spanned by these 12 components. As a result, the worst perturbation Δu satisfying (4.14) can be expressed as a linear combination of *eight* orthonormal basis functions: $\vec{w}=(w_1(x), \ldots, w_8(x))$ with $\|w_n(x)\|_2 = 1$ for $n = 1, \ldots, 8$. Writing $\Delta u = \vec{c}^T \cdot \vec{w}$, where $\vec{c} = (c_1, c_2, \ldots, c_8)$ is a unit vector, one can rewrite the optimization problem as

$$\max_{\vec{c}} \rho(\mathsf{J}) \quad \text{subject to} \quad \|\vec{c}\|_2 = 1. \tag{4.15}$$

This problem can be solved efficiently using an interior-point algorithm [35] with multiple starting points. As an example, Figure 4.1 shows the worst perturbation direction for the soliton $u(x) = \mathrm{sech}(x)$ (i.e., $\omega^* = 0$; note also that here $\|u_s\|_2 = 2$) obtained by solving (4.15). In this case, the minimal noise energy causing convergence failure is found to be $\|\Delta u\|_{2,\min} = 0.97$.

The iterations depend only upon the scaled frequency $\omega^* = \Omega^*/A^*$, and in Figure 4.2 we plot the largest spectral radius $\rho(\mathsf{J})$ for a fixed perturbation-to-signal ratio (PSR), $\|\Delta u\|_2/\|u_s\|_2 = 0.5$, as a function of ω^*. In the figure, $\rho(\mathsf{J})$ reaches its minimal value at $\omega^* = 0$, suggesting that in general the iteration can be made more robust by shifting the soliton frequency to near zero using the Galilean transformation, i.e.,

$$x \to x + \Omega_0 t, \qquad u \to e^{-i\Omega_0 x + i\Omega_0^2 t/2} u. \tag{4.16}$$

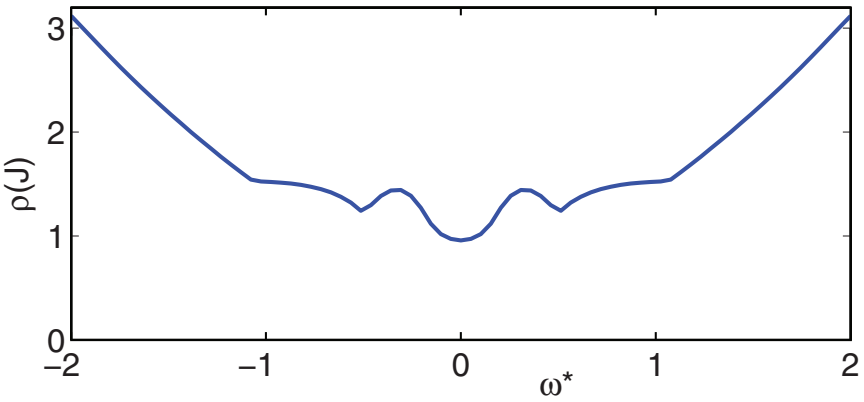

FIG. 4.2. *The largest spectral radius* $\rho(\mathsf{J})$ *as a function of* $\omega^* = \Omega^*/A^*$.

When the transformation is used, the full soliton frequency can be recovered from $\Omega = \Omega' + \Omega_0$, where Ω' is the frequency extracted from the transformed pulse. All of the other soliton parameters remain unaffected, of course.

5. An application: Extracting solitons when ASE noise is present. As an example application of using the functional iteration to extract soliton parameters, consider the case of solitons propagating through an optical fiber with loss compensated by gain from periodically spaced amplifiers [32, 33, 40, 41]. As mentioned previously, the amplifiers add noise to the propagating signal, and this noise is further amplified by subsequent amplifiers.

In dimensionless units, we propagate an initial pulse $u(x, 0) = \mathrm{sech}(x)$ through an optical fiber with 40 amplifiers spaced 0.05 units apart. 256 Fourier modes are used, with a computational window that is 40 units wide. The noise power is assumed to be such that $\sigma^2 = 2 \times 10^{-4}$. Figure 5.1 shows a single pulse perturbed by noise at the output, as well as the soliton extracted from it by using either the iterative method or the ZS eigenvalue problem and the Jost functions. Good agreement is found between the results of the two methods, with the small discrepancy resulting because the pulse obtained from the Jost functions does not have an exact hyperbolic secant shape [33]. For these simulations the iterative method is approximately 20 times faster than solving the ZS problem.

When simulating solitons in the presence of noise one is usually interested in the statistics of the pulses at the output. For this particular example, the total propagation distance is relatively short, and almost all methods produce reasonably good results for the means of the pulse parameters; they are all approximately equal to their initial values. We therefore omit these results here. The one exception to this, however, is that any method that determines the amplitude of the pulse by computing the pulse energy exhibits a mean amplitude that grows with distance; the contribution from the noise cannot be completely eliminated, as described previously.

A more interesting statistic is the variance. Here, we estimated the variance of each of the soliton parameters at all 40 amplifiers using MC simulations with 4000 trials. Again, the initial pulse used is $u(x, 0) = \mathrm{sech}(x)$. In these simulations, the soliton parameters were calculated by both the iterative method and the filtered moment method [33] (because the ZS method is considerably slower than the iterative method and the agreement between the two is good, it was omitted). In Figure 5.2,

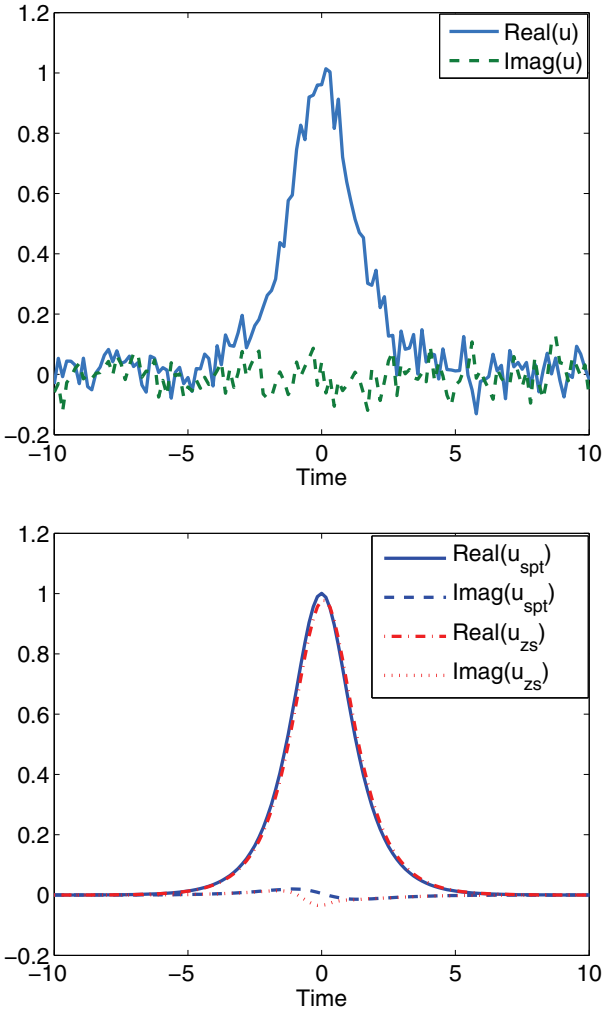

FIG. 5.1. *A noisy pulse (top) and the clean soliton (bottom) recovered by using the iterative method ($u_{\rm spt}$) and by solving the ZS problem ($u_{\rm zs}$).*

we plot the variances of all of the soliton parameters as a function of distance. The analytical estimates for the variance growth obtained with SPT [17, 33] are also shown for comparison:

$$\sigma_A^2 = NA_{\rm o}\sigma^2, \tag{5.1a}$$

$$\sigma_\Omega^2 = 3NA_{\rm o}\sigma^2, \tag{5.1b}$$

$$\sigma_X^2 = N\left[\frac{\pi^2}{12A_{\rm o}^3} + \frac{A_{\rm o}\Delta T^2}{18}(N+1)(2N+1)\right]\sigma^2, \tag{5.1c}$$

$$\sigma_\Phi^2 = N\left[\frac{1}{3A_{\rm o}}\left(1+\frac{\pi^2}{12}\right) + \frac{A_{\rm o}\Delta T^2}{6}(N+1)(2N+1)\right]\sigma^2. \tag{5.1d}$$

Here $A_{\rm o}$ is the initial amplitude (without loss of generality the initial frequency, po-

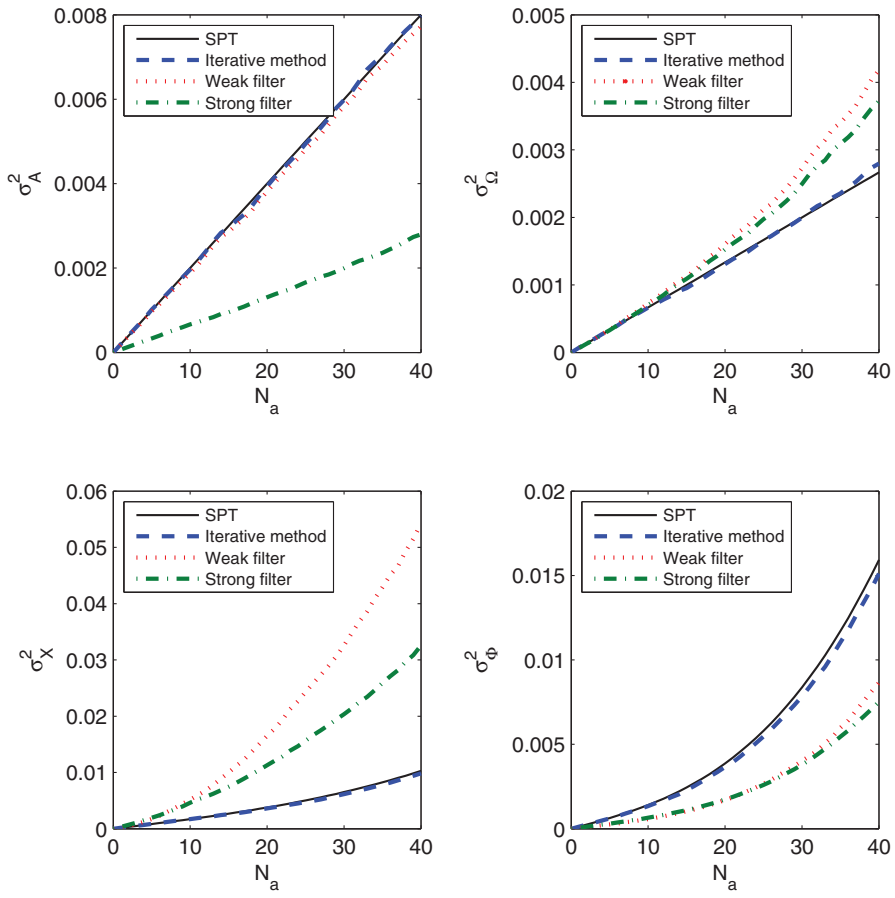

FIG. 5.2. *The variances of the soliton parameters A, Ω, X, and Φ calculated with the iterative method (dashed) or the filtered moment method with either a weak filter (dotted) or a strong filter (dash-dot) as a function of distance. The results predicted from SPT (solid) are included for comparison purposes.*

sition, and phase can be taken to be zero), ΔT is the amplifier spacing, and N is the amplifier number, $N \leq 40$. To better compare the performance of the two methods, we tested two different versions of the filtered moment methods. First, we used the method described in [33] that only filters the pulse in the Fourier domain. Here we used a weak Gaussian filter with a full width at half maximum (FWHM) that is five times that of the pulse, and a strong filter with an FWHM equal to that of the pulse. We also employed a modified version of the filtered moment method described in [33]. In this case, a windowing function in the pulse domain is added to the algorithm: after filtering the pulse in the frequency domain, we first estimate the center of the filtered pulse, $X_{\text{est}} = \int x|u|^2dx / \int |u|^2dx$, and then apply the window

$$G(x) = \exp\left[-\frac{(x - X_{\text{est}})^2}{W^2}\right] \tag{5.2}$$

to the pulse to help remove noise from and beyond the pulse tails. Here W specifies the width of the window function. We used a weak frequency filter (five times the FWHM bandwidth of the pulse) and a weak pulse window (five times the FWHM

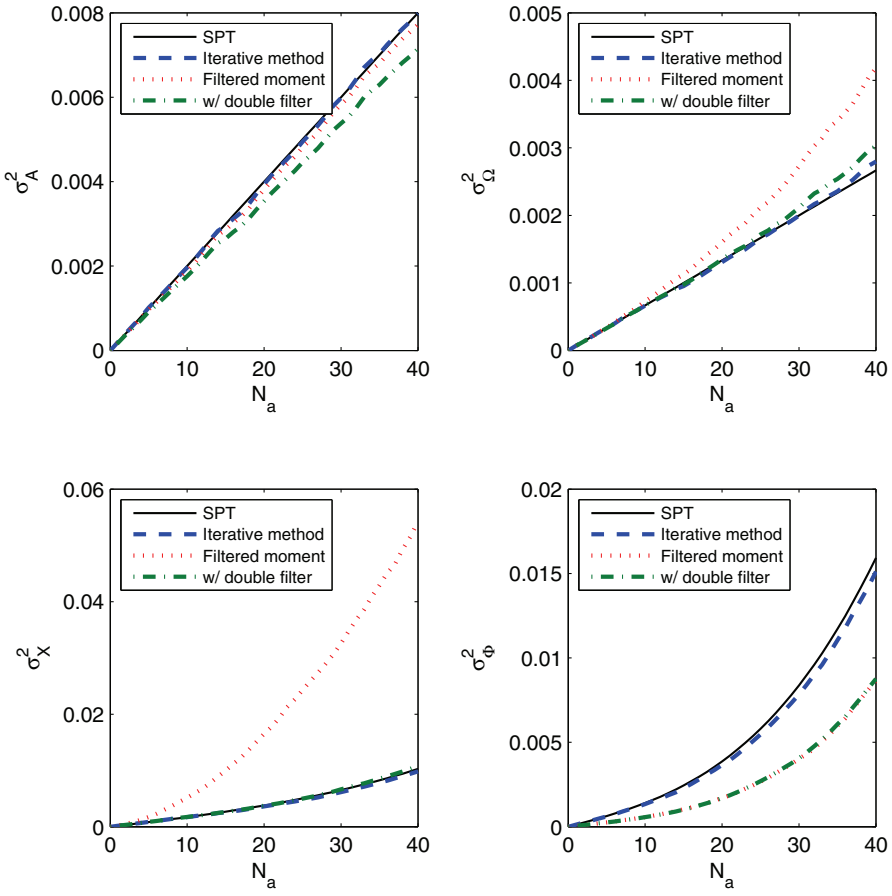

FIG. 5.3. *The variances of the soliton parameters A, Ω, X, and Φ, calculated with the iterative method (dashed), with the filtered moment method with just a frequency filter (dotted), and with filters in both the frequency and pulse domains (dash-dot) as a function of distance. The results predicted from SPT (solid) are again included for comparison purposes.*

width of the pulse). The results are shown in Figure 5.3.

For all of the soliton parameters, the variances obtained with the iterative method agree closely with the analytical predictions. When the moment method with a weak filter is used, only the amplitude variance agrees with the analytical predictions, while the results for all the other parameters depart significantly from the theory. When a stronger filter is used, the results for the frequency and position improve, but those for the amplitude depart even more from the analytical predictions. When filters in both domains are used, the results for the frequency and position become closer to the analytical results, but the pulse windowing causes additional deviations in the amplitude results. Stronger filtering and windowing make these deviations even larger. None of the filtered moment estimations does a satisfactory job for the phase.

6. Conclusions. In summary, we have proposed an efficient and accurate method to extract the underlying soliton from a noisy pulse. The method is based upon SPT and employs a functional iteration to obtain the best-fit pulse parameters. Because analytical perturbation methods are designed to focus on the soliton part of the solu-

tion and ignore the remaining dispersive radiation, an extraction method such as this should be used when one wishes to compare analytical and numerical solutions of the NLSE with perturbations.

We have analyzed the convergence of the method and have shown that its rate of convergence depends upon a single parameter. Furthermore, the analysis shows that when the perturbation is sufficiently small, it converges in all cases. As the size of the perturbation to the pulse grows, however, there is one particular functional direction which most strongly affects the method's convergence, and eventually perturbations in this worst direction cause the method to diverge.

To illustrate the method, we have applied it to determine the statistics of the soliton parameters in the presence of amplifier noise and compared these results with those obtained by the method of moments after filtering the pulse, and also with analytical SPT. The agreement between the current method and SPT is good in all cases. Filtering the pulse and computing its moments can yield good results in some, but not all, cases; in particular, there is always a tradeoff between using a filter that is too weak, leading to results that are impaired by too much noise from dispersive radiation, and using a filter that is too strong that also throws away some of the pulse along with the noise. Even when one filters in both the frequency and pulse domains these tradeoffs are still evident.

Of course, we did not attempt to fully optimize the filter parameters, and thus it might be possible to obtain better results with the moment method in the examples above. If this were the case, however, it would suggest that it could be necessary to optimize the filter parameters under each and every different set of conditions. An advantage of the iterative method described here is that it works well with no adjustable parameters.

We note that the underlying soliton extracted by this method differs from the best soliton approximation of the noisy pulse in the sense of the L_2-norm. For example, the extracted soliton is always of smaller energy than the noisy pulse: since $\langle u_s, \Delta u\rangle = 0$ at the fixed point, one finds $\|u\|^2 = \|u_s+\Delta u\|^2 = \|u_s\|^2+\|\Delta u\|^2$. This is not necessarily the case, of course, if one determines the soliton by minimizing the L_2-norm of the difference between it and the noisy pulse. In addition, while it is generally a difficult task to show that a functional iteration converges to a unique root, from a physical point of view it is easy to understand that, as long as the distortion is not too large, the underlying soliton should exist and be unique. It is possible, of course, for the soliton to be completely destroyed by noise, but the discussion of such large perturbations is beyond the scope of this paper.

Although the method has been developed with the NLSE in mind, it can certainly be extended to other equations with similar properties, e.g., if a full set of modes from the equation linearized around the pulse solution is known. Furthermore, in the case of the NLSE, it should be straightforward to generalize the method to handle more than one soliton and to use it to explore other scenarios, such as a two-soliton collision in the presence of noise. To do so, however, requires not only the analytical two-soliton solution but also the linearized modes associated with it. The appropriate expressions are available or can be computed from known expressions [3], but they are sufficiently cumbersome that one would likely want to have a significant application in mind beforehand that would make the calculation worth the effort.

In addition, at the cost of some additional computational effort the convergence of the method could be improved by modifying the functional iteration so that it becomes Newton's method. Because the functional iteration converges for perturbations with up to almost half of the energy of the soliton, however, the additional effort would

seem justified only in situations where perturbations are extreme. Since for such large perturbations it is reasonable to call into question the original assumption of basing the functional iteration on first-order SPT, however, in such cases soliton extraction based upon the slower but more accurate ZS spectral problem would appear to be the better choice.

Acknowledgments. The authors would like to thank Gino Biondini and Graham Donovan for many interesting discussions about this problem.

REFERENCES

[1] M. J. Ablowitz and T. P. Horikis, *Pulse dynamics and solitons in mode-locked lasers*, Phys. Rev. A, 78 (2008), 011802.
[2] M. J. Ablowitz, T. P. Horikis, S. D. Nixon, and Y. Zhu, *Asymptotic analysis of pulse dynamics in mode-locked lasers*, Stud. Appl. Math., 122 (2009), pp. 411–425.
[3] M. J. Ablowitz and H. Segur, *Solitons and the Inverse Scattering Transform*, SIAM, Philadelphia, 1981.
[4] G. P. Agrawal, *Nonlinear Fiber Optics*, 3rd ed., Optics and Photonics, Academic Press, San Diego, 2001.
[5] G. P. Agrawal, *Fiber-Optic Communication Systems*, 3rd ed., John Wiley & Sons, New York, 2002.
[6] G. Biondini, *The dispersion-managed Ginzburg-Landau equation and its application to femtosecond lasers*, Nonlinearity, 21 (2008), pp. 2849–2870.
[7] S. Burtsev, R. Camassa, and I. Timofeyev, *Numerical algorithms for the direct spectral transform with applications to nonlinear Schrödinger type systems*, J. Comput. Phys., 147 (1998), pp. 166–186.
[8] D. S. Cargill, R. O. Moore, and C. J. McKinstrie, *Noise bandwidth dependence of soliton phase in simulations of stochastic nonlinear Schrödinger equations*, Opt. Lett., 36 (2011), pp. 1659–1661.
[9] C. S. Gardner, J. M. Greene, M. D. Kruskal, and R. M. Miura, *Method for solving the Korteweg-deVries equation*, Phys. Rev. Lett., 19 (1967), pp. 1095–1097.
[10] I. M. Gelfand and S. V. Fomin, *Calculus of Variations*, Prentice-Hall, Englewood Cliffs, NJ, 1963.
[11] J. P. Gordon, *Dispersive perturbations of solitons of the nonlinear Schrödinger equation*, J. Opt. Soc. Amer. B, 9 (1992), pp. 91–97.
[12] K. A. Gorschkov, L. A. Ostrovskii, and E. N. Pelinovsii, *Some problems of asymptotic theory of nonlinear-waves*, Proc. IEEE, 62 (1974), pp. 1511–1517.
[13] A. Hasegawa and Y. Kodama, *Solitons in Optical Communications*, Oxford University Press, Oxford, UK, 1995.
[14] A. Hasegawa and M. Matsumoto, *Optical Solitons in Fibers*, 3rd ed., Springer Series in Photonics, Springer, Berlin, New York, 2003.
[15] A. Hasegawa and F. Tappert, *Transmission of stationary nonlinear optical pulses in dispersive dielectric fibers.* I. *Anomalous dispersion*, Appl. Phys. Lett., 23 (1973), pp. 142–144.
[16] H. A. Haus, W. S. Wong, and F. I. Khatri, *Continuum generation by perturbation of soliton*, J. Opt. Soc. Amer. B, 14 (1997), pp. 304–313.
[17] E. Iannone, F. Matera, A. Mecozzi, and M. Settembre, *Nonlinear Optical Communication Networks*, Wiley, New York, 1998.
[18] E. Isaacson and H. B. Keller, *Analysis of Numerical Methods*, Dover, New York, 1994.
[19] V. I. Karpman and E. M. Maslov, *Perturbation theory for solitons*, Sov. Phys. JETP, 46 (1977), pp. 537–559.
[20] W. L. Kath, *A modified conservation law for the phase of the nonlinear Schrödinger soliton*, Methods Appl. Anal., 4 (1997), pp. 141–155.
[21] D. J. Kaup, *Perturbation theory for solitons in optical fibers*, Phys. Rev. A, 42 (1990), pp. 5689–5694.
[22] D. J. Kaup, *Second-order perturbations for solitons in optical fibers*, Phys. Rev. A, 44 (1991), pp. 4582–4590.
[23] D. J. Kaup and A. C. Newell, *Solitons as particles, oscillators, and in slowly changing media: A singular perturbation theory*, Proc. Roy. Soc. London A, 361 (1978), pp. 413–446.
[24] J. P. Keener and D. W. Mclaughlin, *Green's function for a linear equation associated with solitons*, J. Math. Phys., 18 (1977), pp. 2008–2013.

[25] J. P. Keener and D. W. McLaughlin, *Solitons under perturbations*, Phys. Rev. A, 16 (1977), pp. 777–790.
[26] Y. S. Kivshar and B. A. Malomed, *Dynamics of solitons in nearly integrable systems*, Rev. Mod. Phys., 61 (1989), pp. 763–915.
[27] J. N. Kutz, *Mode-locked soliton lasers*, SIAM Rev., 48 (2006), pp. 629–678.
[28] P. D. Lax, *Linear Algebra and Its Applications*, 2nd ed., Pure Appl. Math. (Hoboken), Wiley-Interscience, Hoboken, NJ, 2007.
[29] J. Li, E. Spiller, and G. Biondini, *Noise-induced perturbations of dispersion-managed solitons*, Phys. Rev. A, 75 (2007), 053818.
[30] B. A. Malomed, *Variational methods in nonlinear fiber optics and related fields*, in Progress in Optics 43, North–Holland, Amsterdam, 2002, pp. 71–193.
[31] C. J. McKinstrie and T. I. Lakoba, *Probability-density function for energy perturbations of isolated optical pulses*, Optics Express, 11 (2003), pp. 3628–3648.
[32] R. O. Moore, G. Biondini, and W. L. Kath, *Importance sampling for noise-induced amplitude and timing jitter in soliton transmission systems*, Opt. Lett., 28 (2003), pp. 105–107.
[33] R. O. Moore, G. Biondini, and W. L. Kath, *A method to compute statistics of large, noise-induced perturbations of nonlinear Schrödinger solitons*, SIAM J. Appl. Math., 67 (2007), pp. 1418–1439.
[34] R. O. Moore, T. Schafer, and C. K. R. T. Jones, *Soliton broadening under random dispersion fluctuations: Importance sampling based on low-dimensional reductions*, Opt. Comm., 256 (2005), pp. 439–450.
[35] J. Nocedal and S. J. Wright, *Numerical Optimization*, 2nd ed., Springer Ser. Oper. Res. Financ. Eng., Springer, New York, 2006.
[36] J. M. Ortega and W. C. Rheinboldt, *Iterative Solution of Nonlinear Equations in Several Variables*, Computer Science and Applied Mathematics, Academic Press, New York, 1970.
[37] E. A. Overman, II, D. W. McLaughlin, and A. R. Bishop, *Coherence and chaos in the driven damped sine-Gordon equation: Measurement of the soliton spectrum*, Phys. D, 19 (1986), pp. 1–41.
[38] A. Quarteroni, R. Sacco, and F. Saleri, *Numerical Mathematics*, Texts Appl. Math. 37, Springer, New York, 2000.
[39] E. T. Spiller, *Computational Studies of Rare Events in Optical Transmission Systems*, Ph.D. thesis, Northwestern University, Evanston, IL, 2006.
[40] E. T. Spiller and W. L. Kath, *A method for determining most probable errors in nonlinear lightwave systems*, SIAM J. Appl. Dyn. Syst., 7 (2008), pp. 868–894.
[41] E. T. Spiller, W. L. Kath, R. O. Moore, and C. J. McKinstrie, *Computing large signal distortions and bit-error ratios in DPSK transmission systems*, Phot. Tech. Lett., 17 (2005), pp. 1022–1024.
[42] J. Stoer and R. Bulirsch, *Introduction to Numerical Analysis*, 3rd ed., Texts Appl. Math. 12, Springer, New York, 2002.
[43] L. N. Trefethen and D. Bau, III, *Numerical Linear Algebra*, SIAM, Philadelphia, 1997.
[44] J. A. C. Weideman and B. M. Herbst, *Finite difference methods for an AKNS eigenproblem*, Math. Comput. Simul., 43 (1997), pp. 77–88.
[45] G. B. Whitham, *Linear and Nonlinear Waves*, Wiley, New York, 1974.
[46] N. J. Zabusky and M. D. Kruskal, *Interaction of solitons in a collisionless plasma and recurrence of initial states*, Phys. Rev. Lett., 15 (1965), pp. 240–243.
[47] V. E. Zakharov and A. B. Shabat, *Exact theory of two-dimensional self-focusing and one-dimensional self-modulation of waves in nonlinear media*, Sov. Phys. JETP, 34 (1972), pp. 62–69.